

# A STELLA Model to Estimate Water and Nitrogen Dynamics in a Short-Rotation Woody Crop Plantation

Ying Ouyang,\* Jiaen Zhang, Theodor D. Leininger, and Brent R. Frey

## Abstract

Although short-rotation woody crop biomass production technology has demonstrated a promising potential to supply feedstocks for bioenergy production, the water and nutrient processes in the woody crop plantation ecosystem are poorly understood. In this study, a computer model was developed to estimate the dynamics of water and nitrogen (N) species (e.g.,  $\text{NH}_4\text{-N}$ ,  $\text{NO}_3\text{-N}$ , particulate organic N, and soluble organic N [SON]) in a woody crop plantation using STELLA (Structural Thinking and Experiential Learning Laboratory with Animation) software. A scenario was performed to estimate diurnal and monthly water and N variations of a 1-ha mature cottonwood plantation over a 1-yr simulation period. A typical monthly variation pattern was found for soil water evaporation, leaf water transpiration, and root water uptake, with an increase from winter to summer and a decrease from summer to the following winter. Simulations further revealed that the rate of soil water evaporation was one order of magnitude lower than that of leaf water transpiration. In most cases, the relative monthly water loss rates could be expressed as evapotranspiration > root uptake > percolation > runoff. Leaching of  $\text{NO}_3\text{-N}$  and SON depended not only on soil N content but also on rainfall rate and duration. Leaching of  $\text{NO}_3\text{-N}$  from the cottonwood plantation was about two times higher than that of SON. The relative monthly rate of N leaching was  $\text{NO}_3\text{-N} > \text{SON} > \text{NH}_4\text{-N}$ . This study suggests that the STELLA model developed is a useful tool for estimating water and N dynamics from a woody crop plantation.

**I**N RECOGNITION OF the potential depletion of fossil fuels within the next several decades and in view of current concerns of elevated carbon dioxide on climate change and other environmental consequences due to the consumption of fossil fuels, the development of renewable energy sources is necessary, and numerous efforts have been devoted to identifying alternatives to fossil fuel sources during the last decade (McKendry, 2002; Galbe and Zacchi, 2002; Berndes et al., 2003). Biomass, the most common form of renewable energy, is biological material derived from algae, agronomic crops, grasses, trees, and municipal waste. Biomass has the potential to become a major global energy source in the next century (Hall, 1997; Kartha and Larson, 2000; Gelfand et al., 2013). Increasing future demand for biomass is likely to include the use of fast-growing hardwoods produced in short-rotation woody cropping systems (Zalesny et al., 2011).

Woody crops can yield energy through the conversion of their biomass into solid, liquid, or gaseous fuels for industrial, commercial, and domestic use. It has been reported that biomass provides about 11% of the world's primary energy supply, and about 55% of the four billion  $\text{m}^3$  of wood consumed annually by the world's population in developing countries is used directly as fuel wood or charcoal to meet daily energy needs for heating and cooking (IEA Bioenergy, 2002). Over the past several decades, short-rotation (3–15 yr) techniques and tree improvement methods have been applied to species such as poplar (*Populus* spp.), willow (*Salix* spp.), and eucalyptus species (*Eucalyptus globulus*) to identify clones selected for their rapid growth, tolerance to pests, and suitability to site conditions to improve biomass production. Poplars have been extensively studied in short-rotation woody biomass production systems (Dickmann et al., 2001; Coleman and Stanturf, 2006; Zalesny et al., 2007). Willow has been selected as an alternative agricultural woody crop grown under short-rotation intensive culture in the northeastern, north-central, and mid-Atlantic regions of the United States (Volk

Copyright © American Society of Agronomy, Crop Science Society of America, and Soil Science Society of America. 5585 Guilford Rd., Madison, WI 53711 USA. All rights reserved. No part of this periodical may be reproduced or transmitted in any form or by any means, electronic or mechanical, including photocopying, recording, or any information storage and retrieval system, without permission in writing from the publisher.

J. Environ. Qual. 44:200–209 (2015)

doi:10.2134/jeq2014.01.0015

Received 11 Jan. 2014.

\*Corresponding author (youyang@fs.fed.us).

Y. Ouyang, USDA Forest Service, Center for Bottomland Hardwoods Research, 100 Stone Blvd., Thompson Hall, Room 309, Mississippi State, MS 39762; J. Zhang, Dep. of Ecology, South China Agricultural Univ., Wushan Rd., Tianhe District, Guangzhou, China; T.D. Leininger, USDA Forest Service, Center for Bottomland Hardwoods Research, 432 Stoneville Rd., Stoneville, MS 38776; B.R. Frey, Dep. of Forestry, Mississippi State Univ., Mississippi State, MS 39762. Assigned to Associate Editor Cole Green Rossi.

**Abbreviations:** ET, evapotranspiration; PON, particulate organic nitrogen; SON, soluble organic nitrogen; STELLA, Structural Thinking and Experiential Learning Laboratory with Animation.

et al., 1999). Eastern cottonwood is a fast-growing poplar and one of the largest native North American hardwoods (Kline and Coleman, 2010). Eucalyptus is among the fastest growing hardwood plantation species throughout the world that can also develop high wood density and thus is being studied for use in large-scale bioenergy production in the southern United States (Gonzalez et al., 2011; Stanturf et al., 2013). Eucalyptus species can accumulate as much as 40 metric tons of dry matter per hectare per year on a wide range of sites in subtropical locations (Sachs et al., 1980).

Several simulation models, such as BIOMASS (McMurtrie et al., 1990), FOREST-BGC (BioGeochemical Cycles) (Running and Coughlan, 1988), and 3-PG (Physiological Principles for Predicting Growth) (Landsberg and Waring, 1997), have been developed to predict biomass production of forests associated with water and nutrient uptake. McMurtrie et al. (1990) developed the process-based BIOMASS model to describe canopy net assimilation, biomass production, and water use of forest stands in relation to weather, tree nutrition, canopy architecture, soil physical characteristics, and physiological variables. BIOMASS has been used to model growth and production in Monterey pine (*Pinus radiata* D. Don) and *Eucalyptus* spp. and was able to predict water use and carbon assimilation of stands. However, N dynamics were not included in the model. Running and Coughlan (1988) developed and applied the FOREST-BGC model to simulate the annual hydrologic balance and net primary production of a hypothetical forest stand in seven contrasting environments. Landsberg and Waring (1997) developed the 3-PG model to simulate forest productivity by calculating radiant energy absorbed by forest canopies and converting it into biomass production. The 3-PG model has been used to predict environmental limitations on growth and final yield of Sitka spruce [*Picea sitchensis* (Bong.) Carrière] stands (Waring, 2000). These models are research tools and have improved our understanding of forest biomass production. However, they are very complicated and require vast amounts of input data, thereby rendering them impractical for wide use by field-based managers and practitioners (Tharakan et al., 2000). These models do not include soil water and N dynamics, which are highly coupled with woody crop biomass production.

Lee and Jose (2005) applied the LEACHM (Leaching Estimation And CHEMistry Model) (Hutson, 2003) to simulate water movement and NO<sub>3</sub>-N fate in the vadose zone of a short-rotation tree plantation. The simulations provide some useful insights on water and NO<sub>3</sub>-N dynamics. The one-dimensional LEACHM tool only estimates water movement and chemical leaching in the unsaturated soil with a daily time step. Surficial processes, such as surface water and fertilizer runoff and tree interactions (e.g., water and nutrient upward movement in the xylem system), are not included. Additionally, the model requires the input of many soil physical properties, such as bulk density, particle size distribution, and water retention characteristics. Because of its daily time step and because it lacks a tree component, LEACHM is unable to simulate the diurnal variations of leaf water transpiration. For estimating diurnal cycles of soil water evaporation, root water uptake, and leaf water transpiration, the hourly time step is required.

In spite of the fact that short-rotation woody crop production technology has demonstrated significant potential for providing feedstocks for bioenergy production, the water and nutrient dynamics associated with possible adverse environmental impacts from short-rotation plantation ecosystems are poorly understood. A more complete knowledge of these processes and of the possible impacts is essential to effective application of this technology. Water movement and the fate and transport of N species in the short-rotation biomass plantation ecosystem are complex processes and are difficult to quantify by field experimentation, due to the variety of short-rotation tree species, for different soil and hydrological conditions and for all possible combinations of surficial driving forces. A need exists to develop a simple yet realistic tool to address the aforementioned issues.

The goal of this study was to develop a STELLA modeling tool to estimate soil water and N species dynamics in a short-rotation woody crop biomass production plantation. The specific objectives of this study were (i) to develop a model component for water dynamics, including surface runoff, rainfall/irrigation, evaporation, percolation, and water uptake by roots on its upward movement from roots through stems to leaves by transpiration; (ii) to develop a model component for soil N dynamics, including mineralization, nitrification, denitrification, sorption, leaching, volatilization, uptake, and fertilizer application; (iii) to calibrate and validate the resulting model using existing experimental data reported by Lee and Jose (2005); and (iv) to apply the calibrated model to estimate water use and N species in the simulated short-rotation biomass plantation ecosystem.

## Materials and Methods

### Model Development

A schematic diagram illustrating the processes involved in water and N dynamics in a short-rotation woody crop biomass production plantation ecosystem, which created the basis for STELLA model development, is shown in Fig. 1. The modeled domain used in this study was 1 ha to a soil depth of 120 cm (Fig. 1C) (Lee and Jose, 2005). Detailed model development approaches are presented below.

### Soil Water and N Dynamics

Soil water dynamics involve runoff, percolation, rainfall/irrigation, and evaporation (Fig. 1A). The surface water runoff (cm<sup>3</sup> h<sup>-1</sup>) is estimated using the following equation (USDA-SCS, 1972; Mullins et al., 1993):

$$\text{Runoff} = \frac{(\text{RI} - 0.2S)^2}{(\text{RI} + 0.8S)} \quad [1]$$

where RI is the rainfall and/or irrigation rate (cm<sup>3</sup> h<sup>-1</sup>), and *S* is the watershed retention parameter, which is estimated by:

$$S = \frac{1000}{\text{CN}} - 10 \quad [2]$$

where CN is the runoff curve number. Curve numbers are a function of soil type, soil physical properties, crop type, and management practices. Surface water runoff occurs only when the rainfall and/or irrigation rate exceeds the infiltration capacity of a soil and surface water ponding occurs. If (RI - 0.2*S*) in Eq.

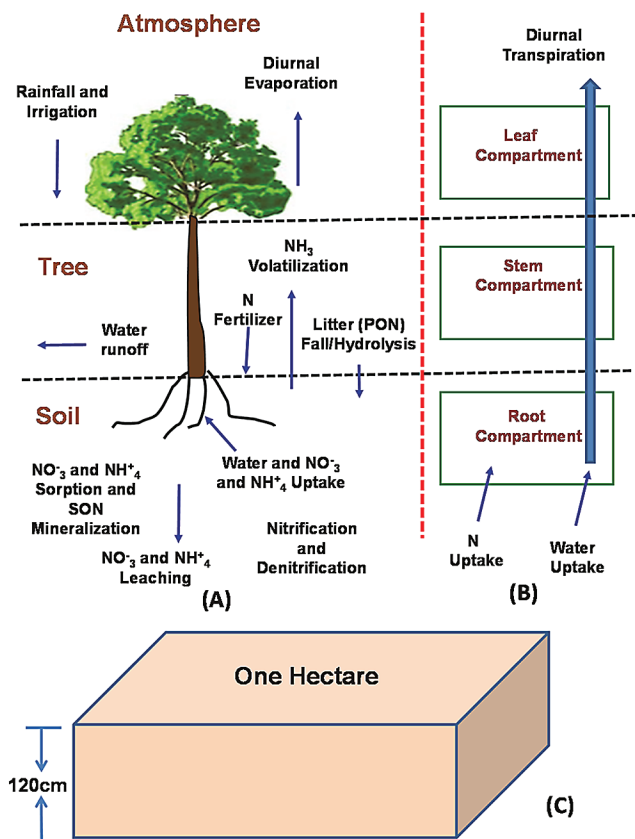


Fig. 1. Schematic diagram showing (A) processes involved in water and N dynamics in a soil–tree–atmosphere system, (B) a compartmental model for water movement and N species uptake within a tree system, and (C) the domain modeled in this study. PON, particulate organic N; SON, soluble organic N.

[2] is negative, the runoff is 0 (USDA–SCS, 1972). Surface water runoff rates can also be measured directly.

The soil water percolation rate is estimated by the following equation (Mullins et al., 1993):

$$Q = \alpha(\theta - f_c) \quad [3]$$

where  $Q$  is the percolation rate ( $\text{cm}^3 \text{h}^{-1}$ ),  $\alpha$  is the drainage coefficient ( $\text{cm}^3 \text{h}^{-1}$ ),  $\theta$  is the volumetric water content ( $\text{cm}^{-3} \text{cm}^{-3}$ ), and  $f_c$  is the field water capacity ( $\text{cm}^{-3} \text{cm}^{-3}$ ). Percolation occurs only when the soil water content is greater than field capacity. Evaporation from soil can be estimated by the Penman–Monteith, Priestley–Taylor equation or by evaporation pan methods (Allen et al., 1989; Abtey and Obeysekera, 1995; Abtey, 1996). Rainfall data can be obtained from local weather stations (Abtey, 1996), whereas irrigation rates are site specific.

Soil N was partitioned into four state variables in this study: particulate organic N (PON), soluble organic N (SON),  $\text{NH}_4\text{-N}$ ,  $\text{NH}_3\text{-N}$ , and  $\text{NO}_3\text{-N}$  (Fig. 1A). More specifically, mechanisms for the fate and transport of N species in a short-rotation woody crop plantation include (i) application of N fertilizer; (ii) volatilization of  $\text{NH}_3\text{-N}$ ; (iii) uptake of  $\text{NO}_3\text{-N}$  and  $\text{NH}_4\text{-N}$ ; (iv) adsorption of SON and  $\text{NH}_4\text{-N}$ ; (v) mineralization of SON; (vi) leaching of SON,  $\text{NH}_4\text{-N}$ , and  $\text{NO}_3\text{-N}$  through the soil; and (vii) transformation of N species. The transformation of N involves the processes of nitrification of  $\text{NH}_4\text{-N}$ , denitrification of  $\text{NO}_3\text{-N}$ , and enzymatic hydrolysis of PON. The  $\text{NO}_2\text{-N}$  concentrations in the soils are unusually low

and only occasionally accumulate in soils and drainage waters (Alexander, 1977; Van Cleemput and Samater, 1995). It was assumed that  $\text{NO}_2\text{-N}$  in the soil from the plantation used in this study is trivial (i.e., all  $\text{NO}_2\text{-N}$  has been converted to  $\text{NO}_3\text{-N}$  or transformed to  $\text{N}_2$ ) (Van Cleemput and Samater, 1995).

The rate of N fertilizer applied to a specific plantation is normally measured during operations. Leaching of N species (i.e., SON,  $\text{NH}_4\text{-N}$ , and  $\text{NO}_3\text{-N}$ ) through the soil can be obtained by

$$L^j = Q C^j \quad [4]$$

where  $L$  is the leaching rate of the N species ( $\text{mg h}^{-1}$ ),  $Q$  is the water percolation rate in the soil ( $\text{cm}^3 \text{h}^{-1}$ ),  $C$  is the concentration of the N species ( $\text{mg cm}^{-3}$ ), and  $j$  denotes the  $j$ th N species. The water percolation rate ( $Q$ ) can be obtained from Eq. [3].

The processes for mineralization, nitrification, denitrification, sorption, leaching, volatilization, uptake, and enzymatic hydrolysis of N can be described by the first-order rate kinetics as (Ouyang et al., 2010):

$$\frac{dS^j}{dt} = k^j S^j \quad [5]$$

where  $S$  is the storage (mg),  $t$  is the time (h), and  $k$  is the first-order rate constant ( $\text{h}^{-1}$ ). All of the first-order kinetics were incorporated into the STELLA model.

### Tree Water Movement and N Uptake

A tree is more complicated geometrically, physiologically, and biologically than the soils of the vadose zone and root zone. Although it is relatively easy to represent water and N transport in the vadose zone, it is extremely difficult to represent transport and fate of water and N in trees using the same concept.

In this study, a STELLA model was developed that separated a generic tree into three compartments of similar structure and function (i.e., the root, stem, and leaf regions) (Fig. 1B). Each compartment should be considered as a transport unit. Compartments were chosen to account for important processes, including water movement from the soil to the atmosphere through the roots, stems, and leaves.

The rate of root water uptake in the soil is primarily controlled by leaf water transpiration. Nobel (1982) stated that about 99% of water taken by roots is used for transpiration and that the remaining 1% is used for tree growth. The uptake of soil water by roots is slightly greater than the loss of tree water due to leaf transpiration. Leaf water transpiration into the surrounding atmosphere depends on tree species, is site specific, and can be estimated by empirical equations (Table 1).

Assuming there is enough soil water available for tree growth, the rate of soil water uptake by roots can be given as:

$$Q_{\text{root}}^{\text{water}} = Q_{\text{leaf}}^{\text{transp}} / 0.99 \quad [6]$$

where  $Q_{\text{root}}^{\text{water}}$  is the soil water uptake rate ( $\text{cm}^3 \text{h}^{-1}$ ), and  $Q_{\text{leaf}}^{\text{transp}}$  is the leaf transpiration rate ( $\text{cm}^3 \text{h}^{-1}$ ).

The rate of N uptake by roots from the soil near the root zone is characterized using the following equation (Ouyang, 2008):

$$R_{\text{rate}}^{\text{root}} = Q_{\text{root}}^{\text{water}} C_{\text{soil}} \delta^{\text{root}} \quad [7]$$

where  $R$  is the rate of  $\text{NO}_3\text{-N}$  and  $\text{NH}_4\text{-N}$  uptake ( $\text{mg h}^{-1}$ ),  $C_{\text{soil}}$  is the soil  $\text{NO}_3\text{-N}$  and  $\text{NH}_4\text{-N}$  concentration ( $\text{mg L}^{-1}$ ), and  $\delta$  the reflection coefficient that measures the metabolic requirement of N to cross into the root compartment. The value for  $\delta$  varies from tree species to species and will be obtained through calibrations and verified through model validations.

## STELLA Model Construction

STELLA is a modeling software package for building a simulating system by creating a pictorial diagram of a model and then assigning the appropriate values and mathematical functions to the system. The major features of STELLA consist of the following four tools: (i) stocks, which are the state variables for storages, act as the sinks (flow in) and sources (flow out) for matter; (ii) flows, which are the exchange variables that control the arrival or the exchanges of information between the state variables; (iii) converters, which are auxiliary variables, can be represented by constant values or by values dependent on other variables, curves, or functions of various categories; and (iv) connectors, which connect among modeling features, variables, and elements. STELLA has been widely used in the biological, ecological, and environmental sciences (Hannon and Ruth, 1994; Peterson and Richmond, 1996; Costanza et al., 2002; Aassine and El Jai, 2002; Ouyang, 2008; Ouyang et al., 2012a, 2012b). A complete description of the STELLA package can be found in Isee Systems (2014).

The first step in STELLA model development is to build a basic structure to capture the processes described in the equations presented above. For instance, the soil water percolation (Eq. [3]) can be translated as shown in Fig. 2. The rectangle is the stock and graphically represents the volume of water stored in the soil. The flow symbol (represented by double lines with arrows and switches) represents the rate that water percolates deeper into the soil profile or out of the stock. The other variables are converters (represented by empty circles) that denote the water content, field capacity, and drainage coefficient. These converters are linked together through connectors (represented by single lines with arrows). The second step is to assign the initial values for stocks as well as equations and input values for flows and converters. With the STELLA model diagram created, the model equations will be generated (Fig. 2B). Figure 3 demonstrates the entire STELLA model developed for water and N species dynamics in the short-rotation woody crop plantation.

## Results and Discussion

### Model Calibration and Validation

Before applying the STELLA model for estimating water and N dynamics in a woody crop plantation, the model needs to be calibrated using one set of observed representative field data and validated using another independent set of observed representative field data. Model calibration involves obtaining

**Table 1. Input parameter values used for model calibration and application.**

Parameter	Value or empirical equation	Source
<b>Water dynamics</b>		
Curve number	81	Nearing et al., 1996
Rainfall, $\text{cm h}^{-1}$	time series measurements	local weather station
Irrigation, $\text{cm h}^{-1}$	0.3	Lee and Jose, 2005
Soil area, $\text{cm}^2$	1,000,000,000 (or 1 ha)	Lee and Jose, 2005
Soil depth, cm	120	Lee and Jose, 2006
Soil porosity, $\text{cm}^3 \text{cm}^{-3}$	0.35	Ouyang et al., 2012a
Field capacity	0.3	Ouyang et al., 2012a
Drainage coefficient, $\text{cm h}^{-1}$	0.005	calibrated
Initial soil water, $\text{cm}^3$	33,600,000,000	calculated
Evaporation coefficient, $\text{cm h}^{-1}$	$-1\text{e-}09 \times \text{time} \times \text{time} + 1\text{e} - 05\text{time} + 0.0017$	estimated from Lee and Jose, 2005
Daily transpiration coefficient, $\text{cm}^3 \text{h}^{-1}$	$-2\text{e-}8 \times \text{time} \times \text{time} + 0.0002 \times \text{time} + 0.032$	estimated from Lee and Jose, 2005
Initial root water, $\text{cm}^3$	2,450,000,000	Lee and Jose, 2006
Initial stem water, $\text{cm}^3$	816,666,667	estimated from Stem volume index (Lee and Jose, 2005)
Initial leaf water, $\text{cm}^3$	816,666,667	Lee and Jose, 2006
Transpiration, $\text{cm}^3 \text{h}^{-1} \text{tree}^{-1}$	0.016	Lee and Jose, 2005
Plant density, trees $\text{ha}^{-1}$	229	Lee and Jose, 2005
Forest cover factor	0.85	assumed
<b>N dynamics</b>		
Initial dissolved SON,† g $\text{ha}^{-1}$	31,200	Ouyang et al., 2010
SON mineralization rate, g $\text{ha}^{-1} \text{h}^{-1}$	0.005	estimated from Lee and Jose, 2006, and Ouyang et al., 2010
Initial dissolved $\text{NH}_4$ , g $\text{ha}^{-1}$	7,500	Lee and Jose, 2006
Initial dissolved $\text{NO}_3$ , g $\text{ha}^{-1}$	1,500	Lee and Jose, 2006
$\text{NH}_4$ nitrification rate, $\text{h}^{-1}$	0.3	estimated from Martin and Reddy, 1997, and Lee and Jose, 2006
$\text{NH}_4$ volatilization rate, $\text{h}^{-1}$	0.00015	Martin and Reddy, 1997
$\text{NH}_4$ adsorption rate, $\text{h}^{-1}$	0.0005	Martin and Reddy, 1997
$\text{NO}_3$ denitrification, $\text{h}^{-1}$	0.005	Martin and Reddy, 1997
Litter enzyme hydrolysis rate, $\text{h}^{-1}$	1.00E-06	Martin and Reddy, 1997
Reflection coefficient	0.001	calibrated

† Soluble organic nitrogen.

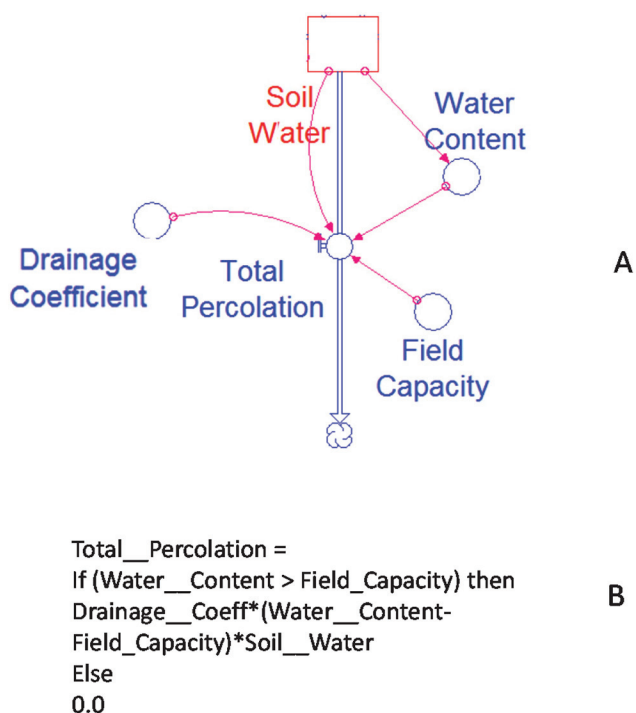


**Fig. 2.** A schematic diagram showing the example translation of soil water percolation process into the STELLA model (A) associated program code (B) that was generated automatically by STELLA. This code describes Eq. [3] and conditions for percolation.

the best fit between the observed data and simulated results by adjusting model input parameter values (Ouyang, 2008). In this study, we attempted to calibrate the model using experimental data reported by Lee and Jose (2005, 2006). These authors studied soil organic N mineralization and  $\text{NO}_3\text{-N}$  leaching in the 7-yr-old cottonwood and loblolly pine plantations grown in a well-drained Redbay sandy loam (a fine-loamy, siliceous, thermic Rhodic Paleudult) in northwest Florida. The mean annual temperature was  $19^\circ\text{C}$ , and the mean annual rainfall was 1700 mm. This sandy loam soil was irrigated  $2 \text{ h d}^{-1}$  at a rate of  $0.3 \text{ cm h}^{-1}$  during the growing season. The  $\text{NO}_3\text{-N}$  fertilizer was applied through a drip irrigation system 0, 56, 112, and  $224 \text{ kg N ha}^{-1}$  per year from June to October. Soil water samples were collected monthly using tension lysimeters installed at 30- and 120-cm soil depths for analyzing  $\text{NO}_3\text{-N}$  and  $\text{NH}_4\text{-N}$ . In our modeling study, we used data for the cottonwood plantation from the treatment with  $56 \text{ kg N ha}^{-1} \text{ yr}^{-1}$ . Table 1 lists all of the input parameter values used for model calibration. These input parameter values were obtained from the experimental measurements by Lee and Jose (2005, 2006) and others (Table 1) or from empirical and theoretical calculations.

To reduce the uncertainties of the model predictions, only two input parameters—the reflection coefficients ( $\delta$ ) in Eq. [7] and the drainage coefficient ( $\alpha$ ) in Eq. [3]—were used for model calibration. The calibration was accomplished by adjusting the values of the reflection and drainage coefficients to match soil water drainage rates and adjusting  $\text{NO}_3\text{-N}$  concentrations from model predictions to match those from experimental measurements Lee and Jose (2005, 2006). Comparisons of the observed and predicted soil drainage and  $\text{NO}_3\text{-N}$  concentration are shown in Fig. 4A and 4B, respectively. The regression equation of the predicted soil drainage against its corresponding

measured soil drainage was  $Y_{\text{Prediction}} = 0.81X_{\text{Measurement}}$  ( $R^2 = 0.76$ ;  $p = 0.0001$ ). The regression equation of the predicted soil  $\text{NO}_3\text{-N}$  concentration against its corresponding measured soil  $\text{NO}_3\text{-N}$  concentration was  $Y_{\text{Prediction}} = 0.98X_{\text{Measurement}}$  ( $R^2 = 0.93$ ;  $p = 1.47\text{E-}07$ ). These values represent reasonably good correlations between the model predictions and the experimental measurements. Visual comparisons of the predicted and observed drainage and  $\text{NO}_3\text{-N}$  concentration as a function of time are shown in Fig. 5; these comparisons demonstrated a close goodness-of-fit graphically.

Model validation is performed to obtain the best fit between the observed data and simulated results without adjusting any input parameter values. In this study, we attempted to validate the drainage and  $\text{NO}_3\text{-N}$  components of the model using an independent set of the experimental data reported by Lee and Jose (2005). More specifically, the drainage and  $\text{NO}_3\text{-N}$  concentration data for model calibration were collected at 120 cm depth, and the drainage and  $\text{NO}_3\text{-N}$  concentration data for model validation were gathered at 30 cm depth. Comparisons of the measured and predicted drainage and  $\text{NO}_3\text{-N}$  concentration are shown in Fig. 4C and 4D. With  $R^2 = 0.95$  and  $p = 0.0008$  for drainage and  $R^2 = 0.93$  and  $p = 1.24\text{E-}07$  for  $\text{NO}_3\text{-N}$  concentration, we concluded that very good agreements were obtained between the model predictions and the experimental measurements during the model validation.

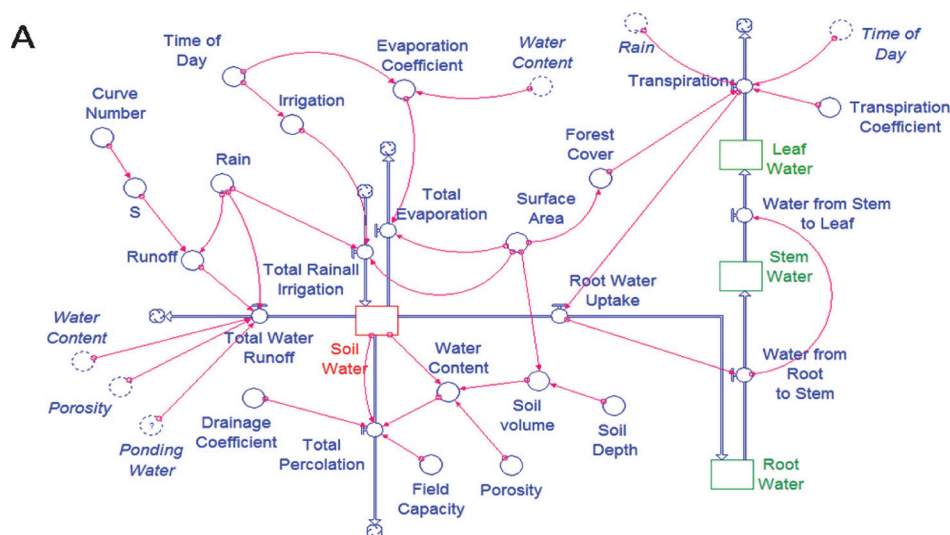
## Model Application

A simulation scenario was performed to gain a better understanding of water and N dynamics in a cottonwood plantation. This scenario investigated (i) diurnal soil water evaporation, leaf water transpiration, and root water uptake in the soil–cottonwood ecosystem; (ii) monthly runoff and percolation of water and monthly leaching of SON and  $\text{NO}_3\text{-N}$  in response to rainfall, irrigation, and fertilization; and (iii) monthly uptake of  $\text{NH}_4\text{-N}$  and  $\text{NO}_3\text{-N}$  by cottonwood and variation of  $\text{NO}_3\text{-N}$  in the soil. A mature (7-yr old) cottonwood plantation with an area of 1 ha and a soil depth of 120 cm was selected as the modeled domain (Fig. 1B), which was similar to the cottonwood treatment at a fertilizer application rate of  $56 \text{ kg N ha}^{-1} \text{ yr}^{-1}$ , as reported by Lee and Jose (2005, 2006). A 1-yr simulation period was chosen for this scenario, which started at 12:00 AM on 1 January and ended on 31 December. The input parameter values used for this scenario are provided in Table 1.

## Diurnal Water Dynamics

Daily variations of soil water evaporation, leaf water transpiration, and root water uptake over a 1-wk (168 h) simulation period are shown in Fig. 6. This figure demonstrates a characteristic diurnal water variation pattern that increased during the day and decreased at night. The diurnal variations of soil water evaporation occurred because of the daily cycle of soil temperature variation, which normally warms during the day and cools at night. The evaporation rate from midnight to 6:00 AM (early morning) was near 0 as a result of cool temperatures. From 6:00 AM to 6:00 PM (sunlight), a large difference in evaporation rate developed due to warm temperatures. For instance, the minimum evaporation rate during the night for the third daily cycle (from 48 to 72 h) was about  $0 \text{ cm}^3 \text{ h}^{-1} \text{ ha}^{-1}$ , whereas the maximum evaporation rate during the day for the same daily

## Soil Water Dynamics Model



## Soil N Dynamics Model

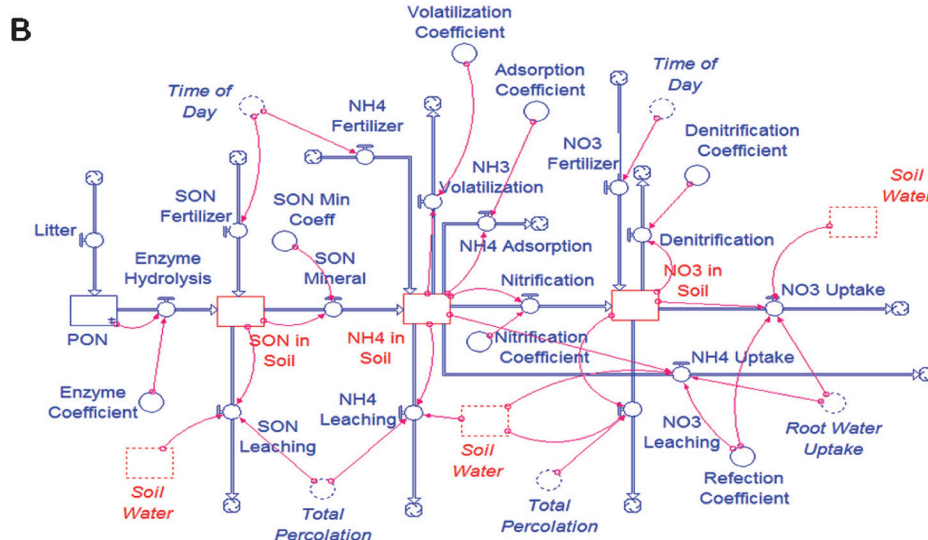


Fig. 3. A STELLA model for soil water (A) and N (B) dynamics in a short-rotation woody crop plantation. PON, particulate organic N; SON, soluble organic N.

cycle was  $169,300 \text{ cm}^3 \text{ h}^{-1} \text{ ha}^{-1}$  (Fig. 6A). Finally, from 6:00 PM (sunset) to 12:00 AM, the evaporation rate decreased to the same level as that from 12:00 AM to 6:00 AM. Starting from the first daily cycle, the evaporation rate increased diurnally during a 1-wk (168-h) simulation period (Fig. 6A). This occurred because soil water evaporation is a seasonal phenomenon and is controlled primarily by soil temperature, which increases from winter to summer and decreases from summer to the following winter. As the soil temperature varies, the soil water evaporation changes accordingly. The empirical equation used to calculate soil water evaporation is given in Table 1 and is formulated based on the data reported by Lee and Jose (2005).

Changes in leaf water transpiration indicated a typical diurnal behavior: an increase during the day followed by a decrease during the night (Fig. 6B). The transpiration rate from 12:00

AM to 6:00 AM was close to 0.0 as a result of leaf stomata being closed at night. From 6:00 AM to 6:00 PM, a dramatic increase in transpiration rate occurred because leaf stomata are open for transpiration during the day. From 6:00 PM to 12:00 AM, the transpiration rate decreased to the same level as that from 0 to 6 h. The maximum transpiration rate during the day for the third daily cycle (from 48 to 72 h) was  $3,195,500 \text{ cm}^3 \text{ h}^{-1} \text{ ha}^{-1}$  (Fig. 6B). This rate was within the range in January reported by Lee and Jose (2005). Analogous to the case of soil water evaporation, leaf water transpiration increased throughout the week. For example, the maximum transpiration rate was  $2,521,200 \text{ cm}^3 \text{ h}^{-1} \text{ ha}^{-1}$  for the first daily cycle but was  $4,044,078 \text{ cm}^3 \text{ h}^{-1} \text{ ha}^{-1}$  for the sixth daily cycle. The latter was about 62% higher than the former. This was consistent with the 54% increase reported by Lee and Jose (2005).

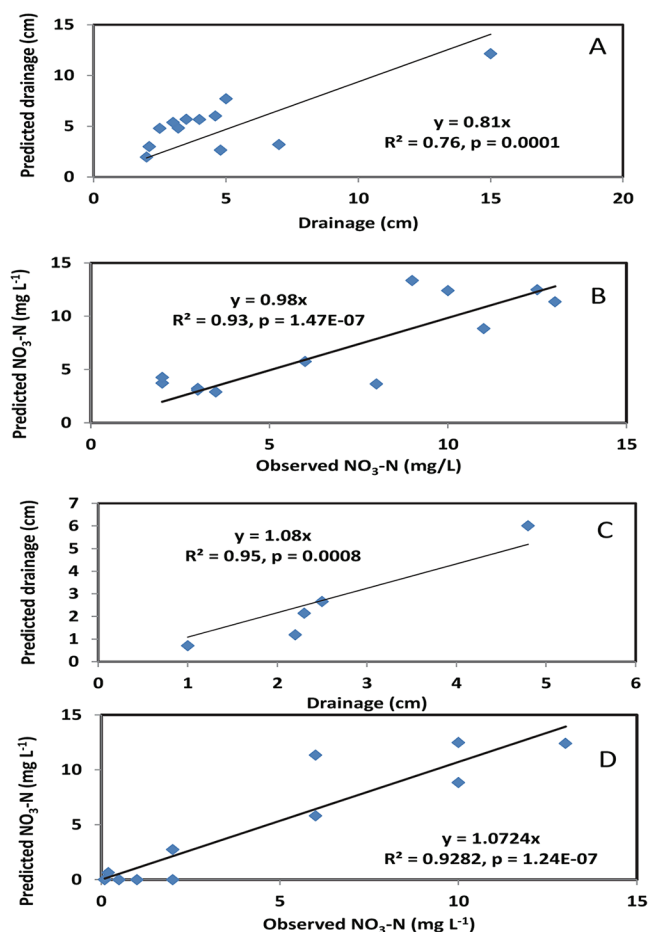


Fig. 4. Comparisons of model predictions with field measurements for soil water drainage (A) and  $\text{NO}_3\text{-N}$  concentrations (B) during the model calibration process as well as for soil water drainage (C) and  $\text{NO}_3\text{-N}$  concentration (D) during the model validation process.

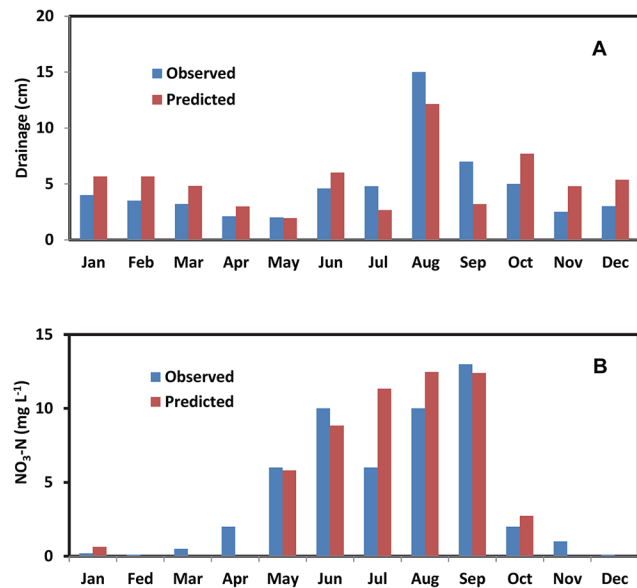


Fig. 5. Comparisons of the predicted and observed monthly drainage (A) and  $\text{NO}_3\text{-N}$  concentration (B).

A similar daily variation pattern was obtained for root water uptake (Fig. 6C). The uptake rate increased from morning to early afternoon and decreased from early afternoon to midnight

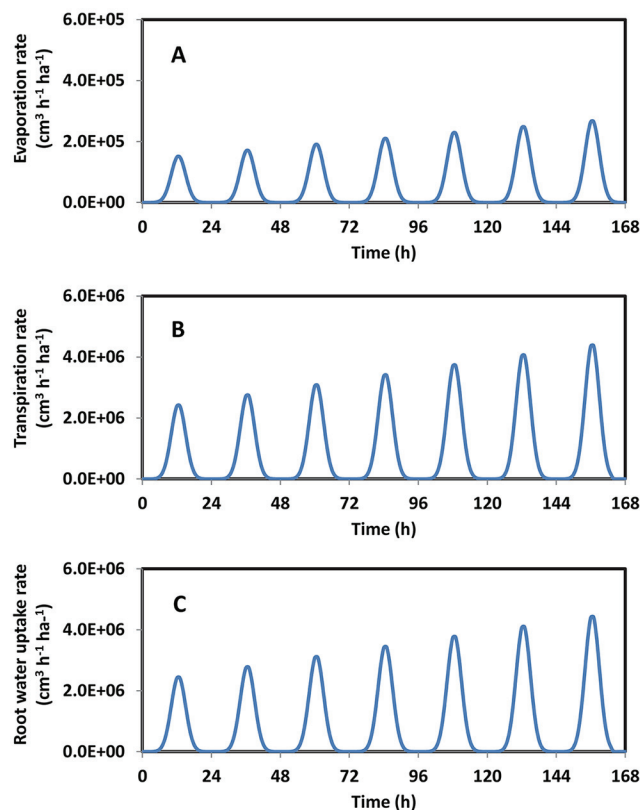


Fig. 6. Predicted diurnal variations of soil water evaporation (A), leaf water transpiration (B), and root water uptake (C).

each day. This daily variation pattern was driven by diurnal leaf water transpiration and was calculated with Eq. [6]. As described in Materials and Methods, the water uptake rate in the soil is primarily controlled by leaf water transpiration. Based on Eq. [6], the uptake of soil water by roots is only slightly higher than the transpiration rate.

Comparison of the rates among soil water evaporation, leaf water transpiration, and root water uptake indicates that the rate of soil water evaporation was one order of magnitude lower than those of leaf water transpiration and root water uptake (Fig. 6). For example, the rate of soil water evaporation was  $274,500 \text{ cm}^3 \text{ h}^{-1} \text{ ha}^{-1}$  for the sixth daily cycle, whereas the rate of leaf water transpiration was  $4,524,500 \text{ cm}^3 \text{ h}^{-1} \text{ ha}^{-1}$  for the same daily cycle. The latter was 16 times higher than the former. This finding was similar to that reported by Lee and Jose (2005, 2006) for the same plantation. Our results revealed that the transpiration of cottonwood leaves played an important role in the daily water cycle. It should be noted that the rates of soil water evaporation and leaf water transpiration are site-specific and vary with plantation locations, soil types, hydrological conditions, and tree species.

## Monthly Water Dynamics

Monthly variations of rainfall/irrigation, surface water runoff, soil water percolation, evapotranspiration (ET), and root water uptake over a 1-yr simulation period are shown in Fig. 7. The rainfall/irrigation data in the figure were the model inputs and were presented for comparison purposes; other data in the figure were the model simulations. There were two major peaks for surface water runoff during the 1-yr simulation, one occurring in

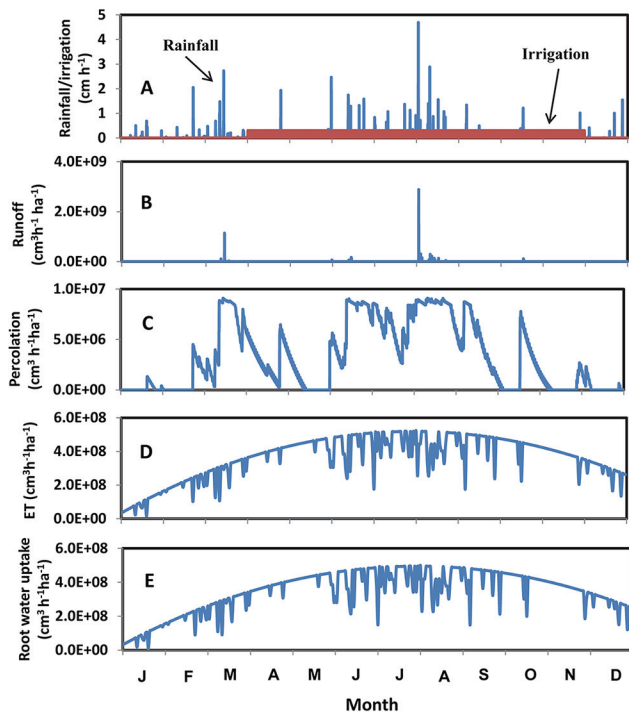


Fig. 7. Monthly variations of rainfall/irrigation (A) and predicted runoff (B), percolation (C), evapotranspiration (ET) (D), and root uptake (E).

March and the other in August (Fig. 7B). These peaks occurred because of two very intensive rainfalls during those 2 mo (Fig. 7A). Surface water runoff occurs when the rainfall and/or irrigation rate exceeds the infiltration capacity of a soil. In this study, the irrigation rate was very small ( $0.3 \text{ cm h}^{-1}$ ) and of short duration (2 h) each day during the growing season (Fig. 7A), and thus surface water runoff was not affected by irrigation.

Two high-percolation periods were observed during the 1-yr simulation. Analogous to the case of surface water runoff, one high-percolation period was near March, and the other occurred during summer (Fig. 7C). The magnitude and duration of the two high-percolation periods corresponded well with rainfall amounts. The maximum percolation rate during August was  $36,401,000 \text{ cm}^3 \text{ h}^{-1} \text{ ha}^{-1}$ . Soil percolation occurred when the soil water content was greater than its field capacity and was highly driven by rainfall and irrigation.

Figure 7D shows the ET rate over a 1-yr simulation period from soil and cottonwoods. This rate had a monthly and seasonal variation pattern. In general, the rate was lower ( $38,320,788 \text{ cm}^3 \text{ h}^{-1} \text{ ha}^{-1}$ ) in early January and higher ( $517,721,988 \text{ cm}^3 \text{ h}^{-1} \text{ ha}^{-1}$ ) in early August. The rate was also related to the duration of rainfall. That is, the ET rate decreased during rainfall primarily due to the cessation of leaf water transpiration during rain events. A similar monthly and seasonal variation pattern was obtained for root water uptake. Root water uptake is mainly controlled by leaf water transpiration. In other words, changes in ET rate were consistent with changes in uptake rate. A comparison of monthly water loss rates among ET, root uptake, percolation, and runoff is shown in Fig. 8A. In most cases, the relative water loss rates within each month occurred in the following order: evapotranspiration > root uptake > percolation > runoff. The ET rate was the sum of the

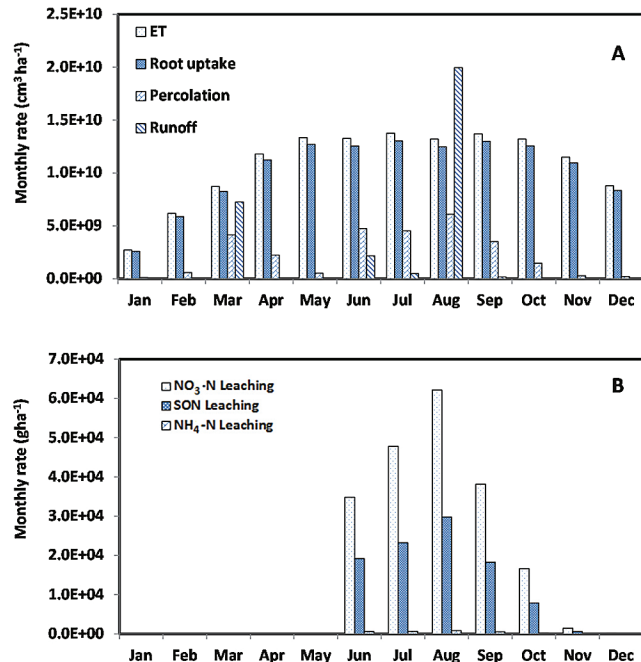


Fig. 8. Predicted monthly water loss rates from evapotranspiration (ET), root uptake, percolation, and runoff (A) as well as predicted monthly leaching rates of  $\text{NO}_3\text{-N}$ , soluble organic N (SON), and  $\text{NH}_4\text{-N}$  (B).

evaporation rate and the transpiration rate. Overall, the rates of monthly water losses were higher during summer and occurred because of the higher ET rate in this season as result of higher soil and air temperatures.

## Soil N Dynamics

Variations in soil  $\text{NO}_3\text{-N}$  and SON leaching and  $\text{NO}_3\text{-N}$  concentration along with rainfall/irrigation over a 1-yr simulation period are shown in Fig. 9. The initial soil  $\text{NO}_3\text{-N}$

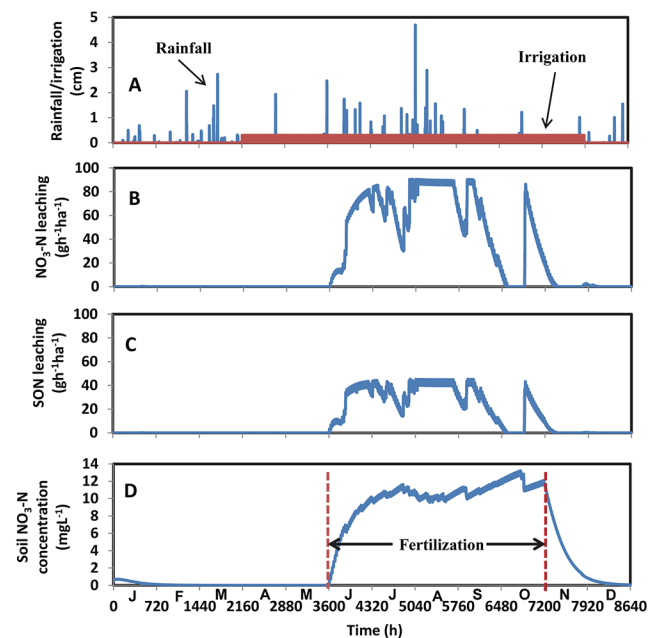


Fig. 9. Variations of rainfall/irrigation (A),  $\text{NO}_3\text{-N}$  leaching (B), soluble organic N (SON) leaching (C), and soil  $\text{NO}_3\text{-N}$  concentration (D) over a 1-yr simulation period.

and  $\text{NH}_4\text{-N}$  concentrations were very low at 0.45 and 0.22  $\text{mg L}^{-1}$ , respectively. Application of N fertilizer (56  $\text{kg N ha}^{-1} \text{ yr}^{-1}$ ) started in June and ended in October (Lee and Jose, 2005). Leaching of  $\text{NO}_3\text{-N}$  deeper into the soil profile was trivial from January to May because of low  $\text{NO}_3\text{-N}$  content in the soil water (Fig. 9B). Starting in June after N fertilizer application, a dramatic increase in  $\text{NO}_3\text{-N}$  leaching occurred, with a maximum of 90  $\text{g h}^{-1} \text{ ha}^{-1}$ . This value was within the range measured in field experiments by Lee and Jose (2005). Figure 8 further reveals that variations in  $\text{NO}_3\text{-N}$  leaching depended not only on soil  $\text{NO}_3\text{-N}$  content but also on rainfall rate and duration. The maximum  $\text{NO}_3\text{-N}$  leaching (Fig. 9B) occurred when the rainfall rate was high in August (Fig. 9A). No  $\text{NO}_3\text{-N}$  leaching was observed when there was no rain in early October even though the soil  $\text{NO}_3\text{-N}$  content was high (Fig. 9D). In addition, the variation pattern in  $\text{NO}_3\text{-N}$  leaching (Fig. 9B) was very similar to that of soil water percolation (Fig. 6C) when the soil  $\text{NO}_3\text{-N}$  content was detectable. This took place because soil percolation was an immediate driving force for  $\text{NO}_3\text{-N}$  leaching. A similar variation pattern was observed for SON leaching (Fig. 9C), although its leaching rate was lower than that of  $\text{NO}_3\text{-N}$ . For example, the maximum leaching rate was about 90  $\text{g h}^{-1} \text{ ha}^{-1}$  for  $\text{NO}_3\text{-N}$  but was about 42  $\text{g h}^{-1} \text{ ha}^{-1}$  for SON. The former was about 2.1 times larger than the latter. We attributed the discrepancy to the mineralization of SON into  $\text{NH}_4\text{-N}$  and the subsequent nitrification of  $\text{NH}_4\text{-N}$  into  $\text{NO}_3\text{-N}$  (Fig. 3B).

Concentration of soil  $\text{NO}_3\text{-N}$  had a different variation pattern (Fig. 9D) as compared with the rates of  $\text{NO}_3\text{-N}$  and SON leaching. After fertilization, the concentration of soil  $\text{NO}_3\text{-N}$  increased continuously and reached its maximum at about 13  $\text{mg L}^{-1}$  in mid-October when there were no soil  $\text{NO}_3\text{-N}$  and SON leaching. Soil  $\text{NO}_3\text{-N}$  concentration depended on its supply (e.g., fertilization and nitrification) and its method of depletion (e.g., leaching, denitrification, and root uptake) (Fig. 3B). In other words, soil  $\text{NO}_3\text{-N}$  concentration was governed not only by soil water percolation but also by the aforementioned factors, which affected the variation patterns. When fertilization stopped, the concentration of soil  $\text{NO}_3\text{-N}$  started to decrease, approaching zero by the end of December.

A comparison of monthly leaching rates among  $\text{NO}_3\text{-N}$ , SON, and  $\text{NH}_4\text{-N}$  is shown in Fig. 8B. The monthly relative N leaching rates occurred in the following order:  $\text{NO}_3\text{-N} > \text{SON} > \text{NH}_4\text{-N}$ . The mechanisms of sorption, volatilization, and nitrification of  $\text{NH}_4\text{-N}$  in the soil are the major reasons for low contents of dissolved  $\text{NH}_4\text{-N}$ , thereby causing a low  $\text{NH}_4\text{-N}$  leaching rate, whereas the mineralization of SON into  $\text{NH}_4\text{-N}$  followed by the nitrification of  $\text{NH}_4\text{-N}$  into  $\text{NO}_3\text{-N}$  resulted in a high  $\text{NO}_3\text{-N}$  leaching rate. No N leaching occurred from January to May or in December because the soil solution N concentrations were not detectable during those months.

## Summary

In this study, a model of soil water and N dynamics within a short-rotation woody crop plantation was developed using STELLA software. The model was calibrated and validated with reasonable agreement between the model predictions and the measured values reported by Lee and Jose (2005, 2006). A simulation scenario was performed to estimate the diurnal and

monthly water and N dynamics from a cottonwood plantation. Although the model was applied to the cottonwood species in this study, it was developed, in general, for any short-rotation woody crops.

A characteristic diurnal variation pattern was observed for soil water evaporation, leaf water transpiration, and root water uptake, with increases from sunrise to early afternoon followed by decreases from early afternoon to sunset. A typical seasonal variation pattern also was found for soil water evaporation, leaf water transpiration, and root water uptake, with increases from winter to summer and decreases from summer to the following winter. Comparison of the rates among soil water evaporation, leaf water transpiration, and root water uptake indicates that the rate of soil water evaporation was one order of magnitude lower than those of leaf water transpiration and root water uptake.

Surface water runoff and soil water percolation were controlled by rainfall rate and duration. In most cases, the relative monthly water loss rates occurred in the following order:  $\text{ET} > \text{root uptake} > \text{percolation} > \text{runoff}$ . Overall, the rates of monthly water losses were higher during summer as expected.

Variations in  $\text{NO}_3\text{-N}$  and SON leaching depended on soil N contents and on rainfall rate and duration. Leaching of soil  $\text{NO}_3\text{-N}$  from the cottonwood plantation was 2.1 times higher than that of soil SON. The relative monthly N leaching rates occurred in the following order:  $\text{NO}_3\text{-N} > \text{SON} > \text{NH}_4\text{-N}$ . Sorption, volatilization, and nitrification of  $\text{NH}_4\text{-N}$  in the soil are the major reasons for the low concentrations of dissolved  $\text{NH}_4\text{-N}$ , which caused a low  $\text{NH}_4\text{-N}$  leaching rate, whereas the mineralization of SON into  $\text{NH}_4\text{-N}$ , followed by the nitrification of  $\text{NH}_4\text{-N}$  into  $\text{NO}_3\text{-N}$ , resulted in a higher  $\text{NO}_3\text{-N}$  leaching rate.

The STELLA model developed in this study was proven to be a useful tool for estimating soil water and N dynamics in the short-rotation woody crop plantations. Knowledge of water use efficiency as well as N fate and transport in plantation systems is crucial to producers and water resource managers, particularly with regards to possible adverse environmental impacts on water quantity and quality when applying short-rotation woody crop biomass production techniques.

The STELLA model was developed to estimate the water and N dynamic processes in a mature woody crop plantation but not in a developing woody crop plantation. Therefore, further study is warranted to add a model component for estimating biomass production in the growing woody crop plantations for a comprehensive understanding of the application of the short-rotation woody crop biomass production technique along with its possible adverse environmental impacts.

## References

- Aassine, S., and M.C. El Jai. 2002. Vegetation dynamics modeling: A method for coupling local and space dynamics. *Ecol. Modell.* 154:237–249. doi:10.1016/S0304-3800(02)00061-3
- Abtew, W. 1996. Evapotranspiration measurements and modeling for three wetland systems in South Florida. *J. Am. Water Resour. Assoc.* 32:465–473. doi:10.1111/j.1752-1688.1996.tb04044.x
- Abtew, W., and J. Obeysekera. 1995. Lysimeter study of evapotranspiration of cattails and comparison of three estimation methods. *Trans. ASAE* 38:121–129.
- Alexander, M. 1977. *Introduction to soil microbiology*. John Wiley & Sons, New York.

- Allen, R.G., M.E. Jensen, J.L. Wright, and R.D. Burman. 1989. Operational estimates of reference evapotranspiration. *Agron. J.* 81:650–662. doi:10.2134/agronj1989.00021962008100040019x
- Berndes, G., M. Hoogwijk, and R. van den Broek. 2003. The contribution of biomass in the future global energy supply: A review of 17 studies. *Biomass Bioenergy* 25:1–28.
- Coleman, M.D., and J.A. Stanturf. 2006. Biomass feedstock production systems: Economic and environmental benefits. *Biomass Bioenergy* 30:693–695.
- Costanza, R., A. Voinov, R. Boumans, T. Maxwell, F. Villa, H. Voinov, and L. Wainger. 2002. Integrated ecological economic modeling of the Patuxent River watershed, Maryland. *Ecol. Monogr.* 72:203–231. doi:10.1890/0012-9615(2002)072[0203:IEEMOT]2.0.CO;2
- Dickmann, D.I., J.G. Isebrands, J.E. Eckenwalder, and J. Richardson. 2001. Poplar culture in North America. NRC Research Press, Ottawa, ON, Canada. p. 206.
- Galbe, M., and G. Zacchi. 2002. A review of the production of ethanol from softwood. *Appl. Microbiol. Biotechnol.* 59:618–628.
- Gelfand, I., R. Sahajpal, X.S. Zhang, R.C. Izaurralde, K.L. Gross, and G.P. Robertson. 2013. Sustainable bioenergy production from marginal lands in the US Midwest. *Nature* 493:514–517. doi:10.1038/nature11811
- Gonzalez, R., T. Treasure, J. Wright, D. Saloni, R. Phillips, R. Abtb, and H. Jameel. 2011. Exploring the potential of eucalyptus for energy production in the southern United States: Financial analysis of delivered biomass: Part I. *Biomass Bioenergy* 35:755–766. doi:10.1016/j.biombioe.2010.10.011
- Hall, D.O. 1997. Biomass energy in industrialized countries: A view of the future. *For. Ecol. Manage.* 91:17–45. doi:10.1016/S0378-1127(96)03883-2
- Hannon, B., and M. Ruth. 1994. *Dynamic modeling*. Springer, New York.
- Hutson, J.L. 2003. LEACHM, model description and user's guide. School of Chemistry, Physics, and Earth Sciences. The Flinders Univ. of South Australia, Adelaide, Australia.
- IEA Bioenergy. 2002. Sustainable production of woody biomass for energy. A position paper prepared by IEA Bioenergy. ExCo 2002; 03. <http://www.ieabioenergy.com> (accessed 18 Oct. 2014).
- Isee System, The World Leader in System Thinking Software. 2014. <http://www.iseesystems.com> (accessed 21 Oct. 2014).
- Kartha, S., and E.D. Larson. 2000. *A bioenergy primer: Modernized biomass energy for sustainable development*. United Nations Development Programme, New York.
- Kline, K.L., and M.D. Coleman. 2010. Woody energy crops in the southeastern United States: Two centuries of practitioner experience. *Biomass Bioenergy* 34:1655–1666. doi:10.1016/j.biombioe.2010.05.005
- Landsberg, J.J., and R.H. Waring. 1997. A generalized model of forest productivity using simplified concepts of radiation-use efficiency, carbon balance and partitioning. *For. Ecol. Manage.* 95:209–228. doi:10.1016/S0378-1127(97)00026-1
- Lee, K.H., and S. Jose. 2005. Nitrate leaching in cottonwood and loblolly pine biomass plantations along a nitrogen fertilization gradient. *Agric. Ecosyst. Environ.* 105:615–623. doi:10.1016/j.agee.2004.08.004
- Lee, K.H., and S. Jose. 2006. Nitrogen mineralization in short rotation tree plantations along a soil nitrogen gradient. *Can. J. For. Res.* 36:1236–1242. doi:10.1139/x06-019
- Martin, J.E., and K.R. Reddy. 1997. Interaction and spatial distribution of wetland nitrogen processes. *Ecol. Modell.* 105:1–21. doi:10.1016/S0304-3800(97)00122-1
- McKendry, P. 2002. Energy production from biomass (part 1): Overview of biomass. *Bioresour. Technol.* 83:37–46.
- McMurtrie, R.E., M.L. Benson, S. Linder, S.W. Running, T. Talsma, W.J.B. Crane, and B.J. Myers. 1990. Water/nutrient interactions affecting the productivity of stands of *Pinus radiata*. *For. Ecol. Manage.* 30:415–423. doi:10.1016/0378-1127(90)90151-Z
- Mullins, J.A., R.F. Carsel, J.E. Scarbrough, and A.M. Ivery. 1993. PRZM-2, a model for predicting pesticides fate in the crop root and unsaturated soil zones: User manual for release 2.0, USEPA, Athens, GA.
- Nearing, M.A., B.Y. Liu, L.M. Risse, and X. Zhang. 1996. Curve number and Green-Ampt effective hydraulic conductivities. *Water Resour. Bull.* 32:125–136.
- Nobel, P.S. 1982. *Biophysical plant physiology and ecology*. Freeman, San Francisco, CA.
- Ouyang, Y. 2008. Modeling the mechanisms for uptake and translocation of dioxane in a soil-plant ecosystem with STELLA. *J. Contam. Hydrol.* 95:17–29. doi:10.1016/j.jconhyd.2007.07.010
- Ouyang, Y., T.D. Leininger, J. Hatten, and P. Parajuli. 2012a. A STELLA model to estimate soil CO<sub>2</sub> emissions from a short-rotation woody crop. *Water Air Soil Pollut.* 224:1392. doi:10.1007/s11270-012-1392-1
- Ouyang, Y., S.M. Luo, and L.H. Cui. 2010. Estimation of nitrogen dynamics in a vertical-flow constructed wetland. *Ecol. Engin.* 37:453–459.
- Ouyang, Y., J.E. Zhang, L.H. Cui, and P. Nkedi-Kizza. 2012b. Simulating the transport and fate of trifluralin in soil. *J. Sustainable Watershed Sci. Manage.* 1:53–60. doi:10.5147/jswsm.2012.0067
- Peterson, S., and B. Richmond. 1996. STELLA research technical documentation. High Performance Systems, Hanover, NH.
- Running, S.W., and J.C. Coughlan. 1988. A general model of forest ecosystem processes for regional applications I: Hydrologic balance, canopy gas exchange and primary production processes. *Ecol. Modell.* 42:125–154. doi:10.1016/0304-3800(88)90112-3
- Sachs, R.M., D.W. Gilpin, and T. Mock. 1980. Short-rotation eucalyptus as a biomass fuel. *California Agriculture* August–September, p. 18–20.
- Stanturf, J.A., E.D. Vance, T.R. Fox, and M. Kirst. 2013. Eucalyptus beyond its native range: Environmental issues in exotic bioenergy plantations. *Int. J. For. Res.*:463030. doi:10.1155/2013/463030.
- Tharakan, P.J., C.A. Nowak, and L.P. Abrahamson. 2000. Modeling growth and biomass production in willow plantations in the northeastern and mid-atlantic United States. *Proceedings of Bioenergy 2000: Moving Technology into the marketplace*. 15–19 Oct. 2000, Buffalo, NY.
- USDA–SCS. 1972. *National engineering handbook*. USDA–SCS, Washington, DC.
- Van Cleemput, O., and A.H. Samater. 1995. Nitrite in soils: Accumulation and role in the formation of gaseous N compounds. *Fert. Res.* 45:81–89. doi:10.1007/BF00749884
- Volk, T.A., L.P. Abrahamson, E.H. White, and M. Downing. 1999. Developing a willow biomass crop enterprise in the United States. In: *proceedings, IEA Task 17 Short-rotation Woody Crops Meeting*. Auburn, GA, 6–9 Sept. 1999.
- Waring, R.H. 2000. A process model analysis of environmental limitations on the growth of Sitka spruce plantations in Great Britain. *Forestry* 73:65–79.
- Zalesny, R.S., Jr., M.W. Cunningham, R.B. Hall, J. Mirck, D.L. Rockwood, J.A. Stanturf, and T.A. Volk. 2011. Woody biomass from short rotation energy crops. In: J.U. Zhu, X. Zhang, and X.J. Pan, editors, *Sustainable production of fuels, chemicals, and fibers from forest biomass*. ACS Symposium Series Vol. 1067. American Chemical Society, Washington, DC, p. 63.
- Zalesny, J.A., R.S. Zalesny, Jr., D.R. Coyle, and R.B. Hall. 2007. Growth and biomass of *Populus* irrigated with landfill leachate. *For. Ecol. Manage.* 248:143–152. doi:10.1016/j.foreco.2007.04.045